High-Throughput Lipophilicity Measurement with Immobilized Artificial Membranes

Bernard Faller,*,† Hans Peter Grimm,‡ Frédérique Loeuillet-Ritzler,† Sabine Arnold,† and Xavier Briand†

Novartis Institutes for BioMedical Research, WSJ-350.3.04, CH-4002 Basel, and GiMS mbH, Maulbeerstrasse 44, CH-4058 Basel

Received August 3, 2004

We report on a new, high-throughput assay designed to measure octanol/water partition coefficients in early drug discovery. The assay is carried out in 96-well microtiterplates and measures the diffusion of compounds between two aqueous compartments separated by a thin octanol liquid layer. Octanol/water partition coefficients are derived from the apparent permeability (P_a) values using a calibration curve. The assay can measure partition coefficients within the range −2 to + 8; thus, a dynamic range of 10 log units can be covered in one single run. Unlike chromatographic methods, the technology is not restricted to neutral and weakly basic compounds, and, as no stationary phase is involved, the data can be strictly compared with values obtained from traditional methods such as shake-flask/HPLC or dual-phase potentiometric titration.

Introduction

The 1-octanol/water partition coefficient ($\log P_{ow}$) has shown to be a useful parameter in quantitative structure−activity relationship.[1,2] The paradigm in today's drug discovery is while the majority of the programs are intended to oral therapy, the use of high-throughput screening techniques and the optimization for binding affinity as a primary target tend to shift leads toward larger, more lipophilic and therefore potentially less soluble compounds.[3] In addition, the improvement of binding affinity during compound optimization is often obtained at the expense of increased lipophilicity. It is therefore important to carefully monitor logP values at the lead selection level and during lead optimization to ensure that the clinical candidates are within an acceptable lipophilicity range. Different approaches such as the shake-flask,[4,5] chromatographic methods,[6−8] the filter probe assay[9] or dual-phase potentiometric titration[10−13] are being used to measure octanol/water partition coefficients. In 2001, Kansy reported on the correlation between lipophilicity and flux through artificial membranes[14] and more recently a linear correlation has been reported between logD and membrane retention at pH 7.4.[15]

Theoretical Basis of the Assay

The geometrical structure of the assay is shown in Figure 1. In a first approximation, it can be assumed that the concentrations in the donor and acceptor compartments (volumes $V_{D/A}$, concentrations $C_{D/A}$) have no spatial variation and that the membrane retention can be neglected. The introduction of the apparent permeability P_a and the membrane-accessible surface area times porosity A leads to the following differential equations:

$$V_D \frac{dC_D}{dt} = -P_a A(C_D - C_A) \quad (1)$$

$$V_A \frac{dC_A}{dt} = +P_a A(C_D - C_A) \quad (2)$$

$$C_D(t = 0) = C_{ini}, \text{ and } C_A(t = 0) = 0$$

The solution of these equations is commonly used to evaluate experimental results, i.e., to determine the membrane permeability ($\log P_a$) from the concentration in the acceptor compartment after a given time lapse t_{end}, $C_A(t = t_{end}) = C_{end}$:

$$P_a - \frac{V_A V_D}{V_A + V_D} \frac{1}{A t_{end}} \ln\left(1 - \frac{C_{end}}{C_{equ}}\right) \quad (3)$$

where

$$C_{equ} = \frac{V_D}{V_A + V_D} C_{ini} \quad (4)$$

Although useful, this treatment proves to be unsatisfactory and even insufficient for a fine-tuned analysis, especially when membrane retention comes into play. Membrane retention refers to the amount of substance which is neither in the donor nor in the acceptor compartment at the end of the incubation time.[16] In fact, to capture the more subtle effects of membrane retention, spatial resolution of the aqueous and the organic phases is necessary. Numerical methods are used to solve the resulting system of partial differential equations (details available as Supporting Information).

Principle of the Method. The method used is derived from the PAMPA technology pioneered by Kansy.[17] Two aqueous compartments are separated by a thin octanol liquid layer coated on a polycarbonate filter. One measures the concentration of the sample in

* To whom correspondence should be addressed. Tel: + 41 61 324 70 90. Fax: + 41 61 324 76 71. E-mail: bernard.faller@pharma.novartis.com.
† Novartis Institutes for BioMedical Research.
‡ GiMS mbH.

10.1021/jm049377w CCC: $30.25
Published on Web 02/19/2005

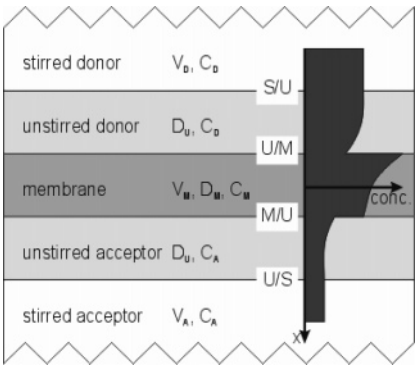

Figure 1. Geometrical structure of the assay. The concentration field in the stack composed of donor, membrane, and acceptor is described with respect to time and the spatial dimension along the axis of the stack, x. Donor and acceptor compartments are further subdivided into an unstirred layer vicinal to the membrane and a stirred zone. The latter is idealized by infinite diffusion leading to a flat solute distribution, whereas the diffusion-limited permeability of the unstirred layer is crucial to the description of nontrivial transients (as shown in the concentration profile). The unstirred layer being very thin as compared to the stirred zone, its volume can be neglected for most considerations. Besides the transport equations inside the respective zones, boundary conditions are imposed at their interfaces for solute conservation and continuity. At the interface of unstirred layers and the membrane, a jump condition is formulated describing the solute distribution (more details are available as Supporting Information).

the acceptor compartment at the end of the 4-hours incubation time, as previously reported in our HDM-PAMPA permeability assay.[18] For hydrophilic compounds ($\log P_{oct} < 0$) the membrane behaves as a barrier while for hydrophobic compounds ($\log P_{oct} > 2$) the apparent permeability is lower than the effective permeability due to membrane retention.[16] As shown in Figure 2, the time-dependent accumulation in the acceptor compartment changes when membrane retention takes place and the apparent permeability (P_a) derived from the concentration at a time t using eq 4 becomes lower than effective permeability (Pe). When membrane retention takes place, the higher the lipophilicity, the bigger the difference between logPe and $\log P_a$. The upper and lower limit of accessible $\log P_{oct}$ values are imposed by the lower limit of quantification in the acceptor compartment.

Results

Diffusion Kinetics in the Presence and Absence of Membrane Retention. Figure 2 shows the theoretical time dependent accumulation in the acceptor compartment of compounds with various lipophilicity values calculated with a water/membrane ratio of 250. The upper panel shows cases where the octanol acts as a barrier while the lower panel shows cases where membrane retention becomes the limiting factor for transport. In the absence of membrane retention, the relation between intrinsic permeability (P_o) and lipophilicity is as follows:[18]

$$\log P_o = \log P_{oct} + \log(D/h) \qquad (5)$$

where D is the diffusion coefficient of the compound within the membrane and h the membrane thickness. When membrane retention takes place two events

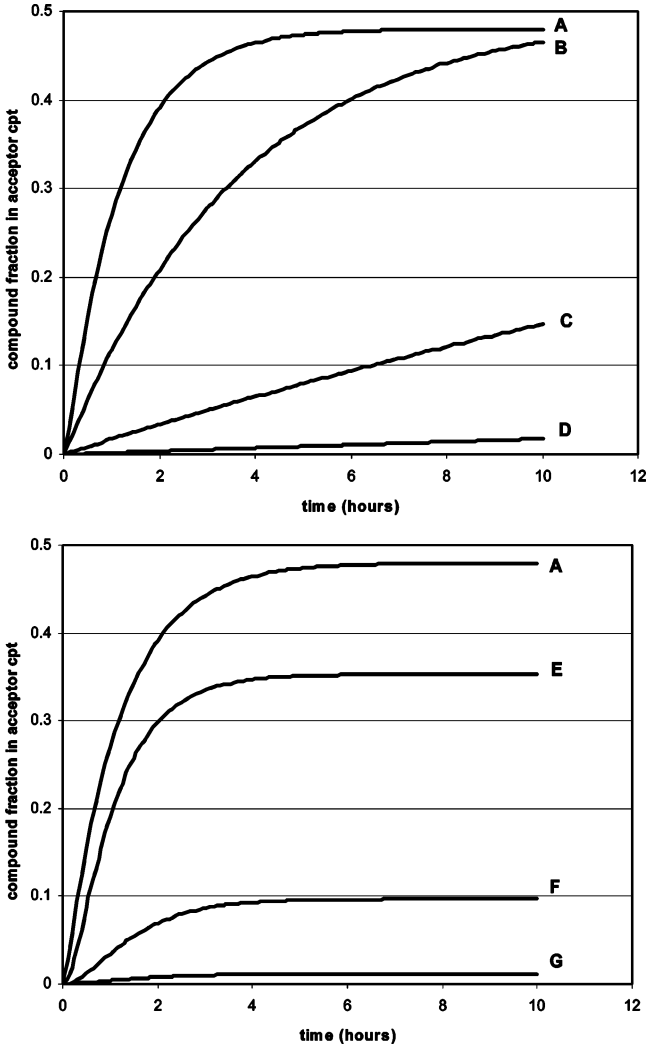

Figure 2. Theoretical concentration vs time profiles in the acceptor compartment calculated for different membrane water distribution coefficients (A: $\log D = 1$, B: $\log D = 0$, C: $\log D = -1$, D: $\log D = -2$, E: $\log D = 2$, F: $\log D = 3$, G: $\log D = 4$). Calculations were performed using a numerical integration approach based on diffusion coefficients in water and membrane. A water/membrane volume ratio of 250 was used with equal donor and acceptor volumes. The absolute concentration in the acceptor compartment is the product of the initial concentration (in donor compartment) times the concentration factor (Y-axis). The upper panel shows situations where the octanol membrane acts as a barrier while the lower panel shows situations where the octanol membrane acts as a trap (membrane retention).

happen: (1) The aqueous concentration decreases as compound gets trapped within the membrane. (2) The shape of the curve is changed as membrane filling induces a pre-steady-state, which translates in a lag time in the kinetics.

Intrinsic Permeability ($\log P_o$) vs Lipophilicity ($\log P_{oct}$). To verify that eq 5 holds in our experimental setup and to estimate the average $\log(D/h)$ ratio for the set of molecules investigated, we measured the intrinsic permeability $\log P_o$ of 10 reference compounds using the pK_a shift technique described previously.[18] In agreement with eq 5, the plot of $\log P_o$ vs $\log P_{oct}$ gives a straight line (Figure 3). From the regression line, it follows that on average, $\log(D/h) = -3.7$ for the set of compounds investigated.

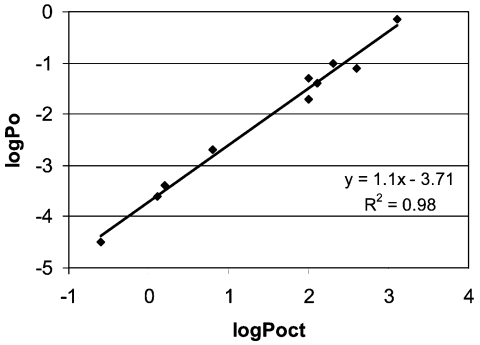

Figure 3. Intrinsic permeability through the octanol membrane vs octanol/water partition coefficient.

Table 1. Influence of Membrane Volume on Effective Porosity and Liquid Layer Thickness

membrane volume (μL)	effective porosity	h (μm)
1.0	0.36	42
1.5	0.44	65
2.0	0.51	84
5.0	0.71	211

Table 2. Calculated Ionization Constants and Derived pH Values Used To Measure Permeability log P_{aN} Values[a]

compound	pK_a ACD	log P_{aN} at pH	log P_{aN}
ganciclovir	9.3 (A)	2, 6	−5.7
famotidine	2.7 (B)−7.9 (B)−10.3(A)	(11)	−4.8
amiloride	3.8 (B)−7.8 (A)	6	−4.4
hydrochlorothiazide	9.0 (A)−9.5 (A)	2, 6	−4.3
sulfamethizole	5.5 (A)	2	−4.0
benzoic acid	4.2 (A)	2	−3.8
furosemide	3.0 (A)−9.8 (A)	2	−4.2
diltiazem	8.9 (B)	11	−4.6
ketoprofen	4.2 (A)	2	−5.1
propranolol	9.1 (A)	2, 6	−5.0
warfarin	4.5 (A)	2	−4.9
valsartan	3.7 (A)− 4.2 (A)	2	−5.7
clozapine	5.3 (B)−7.1 (B)	11	−5.2
nortryptiline	10.1 (B)	11	−6.1
diclofenac	4.2 (A)	2	−5.9
penbutolol	9.2 (B)	11	−5.9
nicardipine	4.3 (B)−7.1 (B)	11	−6.9
chlorpromazine	9.4 (B)	11	−7.0
terfenadine	9.6 (B)	11	−7.6
amiodarone	9.4 (B)	11	−8.7

[a] Acid and base assignments are indicated in brackets. For famotidine, the apparent permeability at pH 11 was used, although the compound is only 50−60% neutral at that pH value (measured pK_a values are 6.7 and 11.2).

Excess Membrane Volume and Apparent Filter Porosity. Nielsen et al.[19] have shown that an excess membrane volume (over the nominal volume of the pores) leads to an increase of the apparent filter porosity. All permeability values were calculated using the apparent permeability coefficients reported in Table 1, which were calculated using a nominal filter porosity of 0.1 and a membrane thickness of 10 μm. Another consequence from the work by Nielsen et al. is that under our experimental conditions, the apparent porosity coefficient is largely influenced by the excess lipid over the nominal volume of the pores. This effect probably masks small changes in nominal filter porosity due to lot to lot variation.

Experimental log P_{oct} Determined from log P_{aN} Values. log P_{aN} refers to the apparent permeability of the neutral species. Table 2 summarizes the log P_{aN} values obtained experimentally with 20 generic drugs covering the log P_{oct} range −2.1 to 7.6. The selection of the pH value where the compounds are >90% neutral was done based on calculated ionization constants using the ACD pK_a DB v7.0 software.

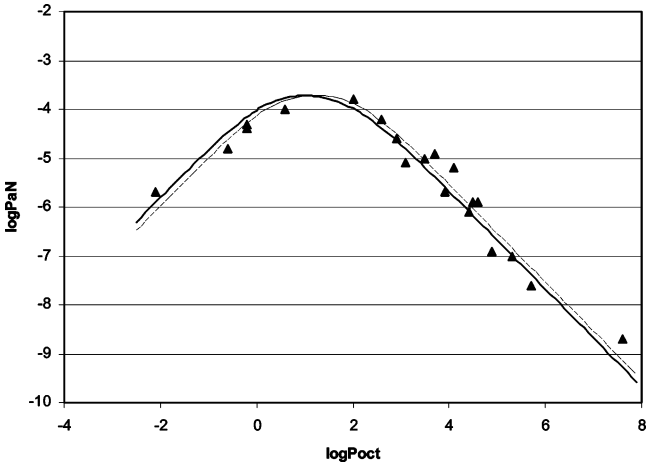

Figure 4. Apparent permeability of the neutral species (log P_{aN}) vs octanol/water partition coefficient (log P_{oct}). The solid line was calculated using the numeric model with log P_{ul} = −3.6, log(D/h) = −3.8, V_d = 0.31 mL, V_a = 0.3 mL, and an effective porosity of 0.51. The dotted line is obtained using the semiempirical eq 6 with $a = 1.1.054 \times 10^{-4}$ and $b = 2.917 \times 10^{-2}$. Triangles show the experimentally measured log P_{aN} values.

Figure 4 shows the experimental log P_{aN} values obtained with increasing log P values. log P_{aN} values were derived from the concentration in the acceptor compartment after 4 h incubation time using eq 3. The solid line in Figure 4 represents the theoretical variation of log P_{aN} with log P_{oct} using the numerical integration approach. The best fit was obtained with log $P_{ul} = -3.6$, log(D/h) = −3.8 (close to the −3.7 derived from Figure 2), and a effective membrane volume of 2 μL. There are several reasons why the effective membrane volume is slightly lower than the effective octanol volume coated on the filter: some octanol dissolves in the buffer (ca. 0.6 μL), while a small fraction (ca. 0.2 μL) evaporates before the sandwich is assembled (see Supporting Information for more information) Permeability−lipophilicity relationships have been described in detail by Kubinyi.[20] The dotted line in Figure 3 is an analytical approximation based on the following semiempirical equation:

$$\frac{1}{P_{aN}} = \frac{1}{P_{ul}} + \frac{1}{aP_o} + \frac{1}{b/P_{oct}} \qquad (6)$$

Equation 6 does not pretend to have a physical meaning. It is a semiempirical analytical expression which links apparent membrane permeability (log P_{aN}) to lipophilicity (log P_{oct}). The first term represents the contribution of unstirred water layer, the second the membrane barrier, and the third the membrane retention effect. Equation 6 can be rearranged into a quadratic equation for P_{oct}, i.e. for any value of $P_{aN} < P_{aN}^{max}$ two solutions for P_{oct} are obtained. One then makes use of CLOGP to distinguish which of the two solutions is the relevant one. The best fit to the experimental data using eq 6 was obtained with $a = 1.054 \times 10^{-4}$ and $b = 2.917 \times 10^{-2}$.

Parameter Sensitivity Analysis. We have used numerical integration to investigate the impact of the

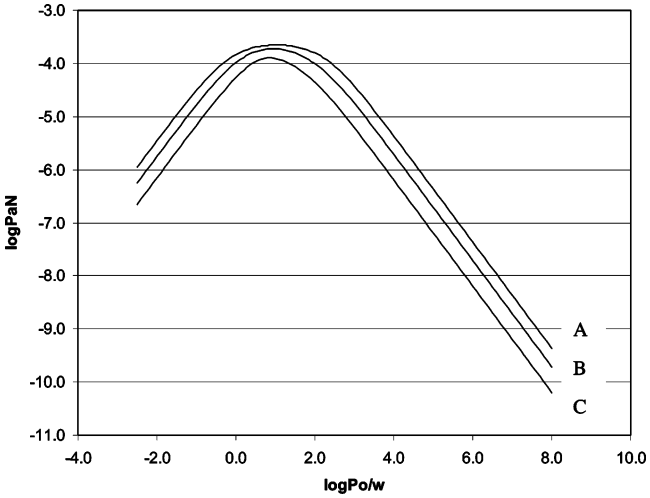

Figure 5. Influence of membrane volume on log P_{aN} vs octanol/water partition coefficient. Curve A (1 μL), B (2.0 μL), C (5 μL). Curves A−C were calculated using the numeric approach using the parameters from Table 1.

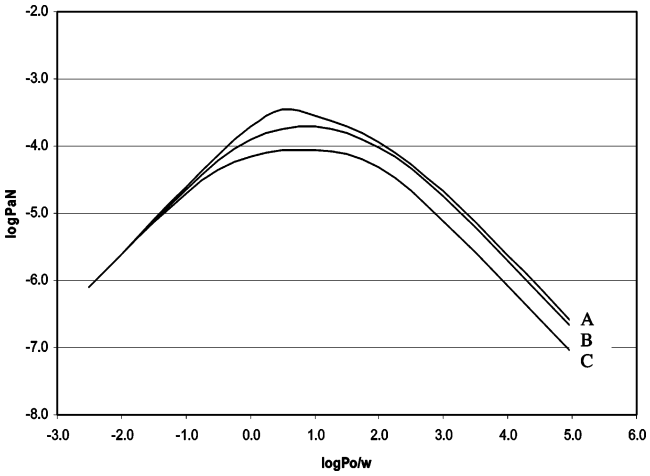

Figure 6. Effect of stirring efficiency on the apparent permeability vs lipophilicity plot. log $P_{ul} = -3.0$ (curve A), −3.6 (curve B), −4.0 (curve C).

variation of key parameters on the assay results (see Supporting Information for additional details about the procedure). Figure 5 shows the effect of variation of membrane volume on the log P_{aN} vs log P_{oct} plot. For log P_{oct} values below 1, log P_{aN} values are shifted to lower values because log(D/h) decreases as membrane volume increases while the same pattern is observed for higher log P_{oct} values, but this time caused by membrane retention.

Figure 6 shows the effect of change in log P_{ul} on the log P_{aN} vs log P_{oct} curve. Variations in log P_{ul} could for example be achieved by changing the stirring conditions during the incubation time. One can see that with lower log P_{ul} values (larger boundary layers), log P_{aN} does not change much with varying log P_{oct} within the range 0−1.5; thus lowering the accuracy of the method.

HT-log P_{ow} vs Calculated log P_{ow}. Table 3 shows the reference log P_{oct} values vs calculated and HT-log P_{oct} values (this paper), which were obtained by extracting log P_{oct} from log P_{aN} using eq 6. Statistical analysis of the data in Table 3 shows that the HT-logP method gives a standard deviation of 0.31 while CLOGP gives a standard deviation of 0.59 with the set of generic drugs

Table 3. Comparison between Calculated log P, High-Throughput log P (this work), and Reference Values[a]

compound	CLOGP	log P_{oct}	HT-log P
ganciclovir	−2.5	−2.1 (a)	−1.8
famotidine	−0.6	−0.8 (b)	−0.8
amiloride	0.1	−0.2 (a)	−0.4
hydrochlorothiazide	−0.36	−0.2 (a)	−0.2
sulfamethizole	0.42	0.6 (a)	0.3
benzoic acid	1.9	2.0 (a)	1.5
furosemide	1.9	2.6 (b)	2.5
diltiazem	3.6	2.9 (b)	3.0
ketoprofen	2.7	3.2 (b)	3.5
propranolol	2.7	3.5 (b)	3.4
warfarin	2.9	3.7 (a)	3.3
valsartan	4.8	3.9 (a)	4.1
clozapine	3.7	4.1 (b)	3.6
nortryptiline	4.3	4.4 (b)	4.5
diclofenac	4.7	4.5 (b)	4.4
penbutolol	3.6	4.6 (a)	4.4
nicardipine	5.2	4.9 (a)	5.4
chlorpromazine	5.3	5.4 (b)	5.5
terfenadine	6.1	5.7 (a)	6.1
amiodarone	8.9	7.6 (b)	7.2

[a] HT-log P values were calculated from the log P_{aN} values in Table 1 and converted to log P values using eq 18. Referenced log P_{oct} values were either measured in-house (a) using dual-phase potentiometric titration, except for ganciclovir which was measured by shake-flask/HPLC, or obtained from literature (b) (refs 22, 23).

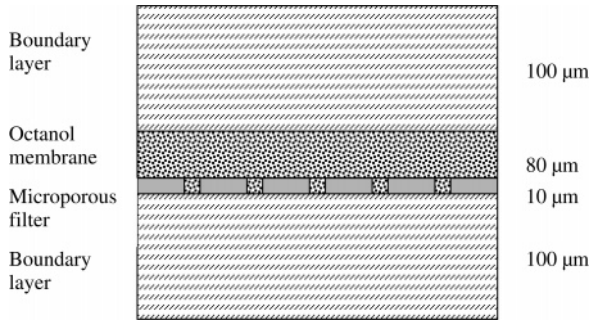

Figure 7. Macroscopic representation of the octanol filter-coated membrane.

tested. Our experience is that the prediction software performs less well with new, lead optimization compounds than with known drugs, and therefore the difference is expected to be greater in a real drug discovery setup.

Geometrical Structure of the Octanol Membrane. We have used the various parameters measured with the reference compounds to propose a geometrical structure of the membrane main components (Figure 7). If one assumes an average diffusion coefficient in water of 5×10^{-6} cm^2 s^{-1} and the measured P_{ul} of $10^{-3.6}$, one gets a thickness for the boundary layers at the donor and acceptor side of 200 μm. The thickness of the membrane was estimated from the effective octanol volume (2 μL) coated on a 0.237 cm^2 filter surface and gives a value of 80 μm. One comes to a similar value if one starts from the experimentally determined D/h value of $10^{-3.7}$ (Figure 3) and assumes an average ratio of diffusivities in octanol to water of 4.

Discussion

We have developed an alternative approach for log P_{oct} determination based on artificial liquid membrane permeability in 96-well plates. The method works with neutral, acidic, and basic low molecular weight com-

pounds. Calculated or measured pK_a values are used to determine at which pH the compound fraction is >90% neutral. log P_{aN} (apparent permeability of the neutral species) is then used to calculate back the membrane log P partition coefficient. This way, one calibration curve covers neutral, acidic, and basic compounds. In contrast to RP-HPLC-based methods, the method presented here measures log P (partition coefficient) while the other techniques measure log D (distribution coefficient) values. log P_{oct} values can easily be converted into log D if the ionization constants are known. High-throughput measurement of ionization constants has been recently described;[21] alternatively, one can rely on calculated values, depending on the accuracy needed and the chemical space investigated. Potentially, the method can be relatively easily extended to other water/solvent systems. The limitation of the approach is with some ampholytes and zwitterions, which are never >90% neutral at any pH value throughout the range 2−11 and for which only an approximated log P_{oct} value can be derived.

The measurement of apparent permeability values through an octanol liquid membrane is an effective way to access a broad dynamic range of log P_{oct} values, from −2 to + 8 in one single experiment. The technique is relatively simple, and the assay format is easily compatible with traditional laboratory robotics. The assay dynamic range is best when LC-MS is used as a detection system (−2 to +8), although it is also possible to use UV detection to quantify the compound concentration in the acceptor compartment. According to our experience, the dynamic range with UV detection is slightly reduced toward to the very lipophilic compounds with a dynamic range from −2 to +5. In addition, the assay is very well suited to measure lipophilicity of low-soluble compounds, as it easily works with low sample concentrations. In this context, one should note that amiodarone was loaded above its intrinsic solubility, even though the incubation is performed in the presence of 5% (v/v) DMSO. A fraction of amiodarone has most certainly precipitated in the reference solution (prepared at 0.02 mM). In the sandwich construct, the precipitation is minimized due to the partitioning of the compound into the organic phase. This is most likely why the log P_{aN} value of amiodarone is slightly overestimated and above the line in Figure 4.

The assay leads to less accurate log P_{oct} values in two cases: (1) within the log P_{oct} 0 to 2, because the variation of log P_{aN} with log P_{oct} flattens; (2) when the compound neutral fraction is never >90% throughout the pH range 2−11. This is typically the case for some ampholytes and for zwitterions.

Another limitation inherent to the approach is that it assumes that the diffusion coefficient (D) stays relatively constant among the molecules tested and between the training and the test set. In practice, this is not an issue for the screening of low molecular weight compounds usually synthesized in medicinal chemistry programs.

In conclusion, the OCT-PAMPA assay provides relatively accurate log P_{oct} value, which can be directly compared to values obtained using traditional, labor intensive techniques. It does not require any special instrumentation and can therefore be used in small and medium size companies as well as in academic laboratories. The method can potentially be extended to other water/partition solvent systems.

Experimental Methods

Reagents. All generic drugs were purchased from Sigma (Div. of Fluka Chemie AG, Buchs, Switzerland) except Valsartan (Diovan), which was synthesized in-house. Compounds were dissolved in dimethyl sulfoxide (DMSO) at a concentration of 10 mM each and used without further purification. DMSO was purchased from Merck AG (Dietikon, Switzerland) with a purity grade >99.8%. Hexane (Merck 1.04367) and octanol (Riedel-de-Haën 24134) were with purity grades >99% and >98%, respectively.

OCT-PAMPA Experiments. Permeation experiments are carried out in 96-well microtiter filter plates obtained from Millipore AG (Volketswil, Switzerland). Filter (Isopore, polycarbonate) specifications are as follows: 0.2 μm pore size, 9−10 μm thickness, and 8% porosity. Each well of the filter plate is impregnated with 5 μL of 60% octanol dissolved in hexane (i.e., total amount of octanol/well: 3 μL) for 15 min to allow a complete evaporation of hexane. Subsequently, the donor compartments are hydrated with 300 μL of 0.04 mM of test compound in buffer, containing 4% DMSO, and connected to a homemade Teflon acceptor plate which had been prefilled with buffer containing 4% DMSO. The resulting sandwich construct is incubated at room temperature under constant shaking (150 rpm). After 4 h, the sandwich is disassembled and the solution in the acceptor is transferred to a disposable polystyrene plate and loaded to the LC-MS autosampler.

To ensure that the donor/acceptor fluxes are not due to porous or unstable octanol layers, the stability of the membranes is tested at the end of the incubation time by electrical resistance measurements. Electrical resistance measurements are performed using a Keithley 6517A electrometer (Keithley Instruments S.A., Dübendorf, Switzerland) with Ag/AgCl electrodes from World Precision Instruments (Berlin, Germany). Wells with barriers which displayed electrical resistance lower than 5 kOhm are discarded.

Each compound was measured in triplicate at pH 2.0, 6.0, and 11.0. Buffers used were 20 mM phosphate (Fluka ref 60220), 20 mM MES (Sigma ref M-8902), and 20 mM phosphate (Fluka ref 60220) + 20 mM CAPS (Sigma ref. C-2682), respectively. The final pH was adjusted by the addition of concentrated KOH or HCl.

LC-MS System. The LC-MS analyses were performed with an Agilent 1100 series LC system with two binary pumps and a MSD SL quadrupole detector equipped with an electrospray ionization (ESI) source (Agilent Technologies, Waldbronn, Germany). Nitrogen was used as nebulizer gas at 40 psi and as drying gas at a flow rate of 12 l/min at 350 °C. The capillary voltage is set at 3 kV. The chromatographic desalting step is achieved with a gradient on Chromolith Flash RP-18e (25 × 4.6 mm, Merck, Germany). The mobile phase is composed of a mixture of acetonitrile and water. Formic acid (0.2% v/v) is added in positive mode and 1 mM of ammonium acetate in negative mode. Pumps are operated at 0.5 mL/min during sample analysis and at 1 mL/min during the regeneration step. Columns are maintained at 35 °C in an oven to prevent variation in retention time. The use of two chromatographic pumps allows an injection every 3 min.

Sample Preparation. Compounds are initially loaded in the donor compartment at 0.04 mM and at their theoretical equilibrium concentration (0.02 mM) in the reference plate. At the end of the assay, 10 μL of formic acid 4% (v/v) is added to the pH 11 wells to neutralize the solution. This operation is performed to prevent compound degradation, through long exposure to an alkaline medium and avoid repeated loading of alkalis on the stationary phase. Prior to injection, references are diluted 10 times by the autosampler to avoid saturation of the detector while maximizing the sensitivity and thus the dynamic range of the assay.

A 30 μL volume of each sample is used to load a 20 μL injection loop and analyzed in single ion scan mode using the

molecular mass of the lowest isotope of the compound of interest. Each sample is quantified by comparing the peak surface area of the analyte with a reference at the same pH.

Acknowledgment. The authors thank Millipore Corp., Danvers, MA, for providing special 96-well filter plates with associated technical information.

Supporting Information Available: Transport equations and boundary equations as well as details on the numerical model used to calculate curves displayed in Figures 2 and 4. Measurements of the solubility of octanol in the aqueous media in the presence and absence of 5%. This information is available free of charge via the Internet at http://pubs.acs.org.

References

(1) Leo, A.; Hansch, C.; Church, C. Comparison of parameters currently used in the study of structure−activity relationships. *J. Med. Chem.* **1969**, *12*(5), 766−771.
(2) Hansch, C.; Bjoerkroth, J. P.; Leo, A. Hydrophobicity and central nervous system agents: on the principle of minimal hydrophobicity in drug design. *J. Pharm. Sci.* **1987**, *76*(9), 663−687.
(3) Lipinski, C. A. Drug-like properties and the causes og poor solubility and poor lipophilicity. *J. Pharmacol. Toxicol. Methods* **2000**, *44*, 235−249.
(4) Fujita, T.; Iwasa, J.; Hansch, C. A new substituent constant, π, derived from partition coefficients. *J. Am. Chem. Soc.* **1964**, *86*(23), 5175−5180.
(5) Leo, A.; Hansch, C.; Elkins, D. Partitioncoefficients and their uses. *Chem. Rev.* **1971**, *71*(6), 525−616.
(6) Mirrlees, M. S.; Moulton, S. J.; Murphy, C. T.; Taylor, P. J. Direct measurement of octanol−water partition coefficients by high-pressure liquid chromatography. *J. Med. Chem.* **1976**, *19*(5), 615−619.
(7) Minick, D. J.; Frenz, J. H.; Patrick, M. A.; Brent, D. A. A comprehensive method for determining hydrophobicity constants by reversed-phase high-performance liquid chromatography. *J. Med. Chem.* **1988**, *31*(10), 1923−1933.
(8) Lombardo, F.; Shalaeva, M. Y.; Tupper, K. A.; Gao, F.; Abraham, M. H. ElogPoct: A Tool for Lipophilicity Determination in Drug Discovery. *J. Med. Chem.* **2000**, *43*(15), 2922−2928.
(9) Tomlinson, E. Filter-probe extractor: a tool for the rapid determination of oil−water partition coefficients. *J. Pharm. Sci.* **1982**, *71*(5), 602−604.
(10) Clarke, F.; H.; Cahoon, N. M. Ionization constants by curve fitting: determination of partition and distribution coefficients of acids and bases and their ions. *J. Pharm. Sci.* **1987**, *76*(8), 611−620.
(11) Avdeef, A. pH-metric log P. Part 1. Difference plots for determining ion-pair octanol−water partition coefficients of multiprotic substances. *Quant. Struct.−Act. Relat.* **1992**, *11*(4), 510−517.
(12) Avdeef, A. pH-Metric log P. II. Refinement of partition coefficients and ionization constants of multiprotic substances. *J. Pharm. Sci.* **1993**, *82*(2), 183−190.
(13) Slater, B.; McCormack, A.; Avdeef, A.; Comer, J. E. A. pH-Metric log P. 4. Comparison of Partition Coefficients Determined by HPLC and Potentiometric Methods to Literature Values. *J. Pharm. Sci.* **1994**, *83*(9), 1280−1283.
(14) Kansy, M.; Fischer,. H.; Kratzat, K.; Senner, F.; Wagner, B.; and Parilla, I. High-Throughput Artificial Membrane Studies in Early Lead Discovery and Development. In *Pharmacokinetics Optimization in Drug Research*; Testa, B.; van de Waterbeemd, H.; Folkers, G.; Guy, R.; Eds.; Verlag Helvetica Acta: Zürich and Wiley-VCH: Weinheim, 2001; pp 447−464.
(15) Avdeef-A. *Absorption and Drug Development: Solubility, Permeability and Charge State*; John Wiley & Sons: New York, 2003; pp 153−171.
(16) Avdeef, A.; Strafford. M.; Block. E.; Balogh. M. P.; Chambliss, W.; Khan. I. Drug absorption in vitro model: filter-immobilized artificial membranes 2. Studies of the permeability properties of lactones in Piper methysticum Forst. *Eur. J. Pharm. Sci*. **2001**, *14*, 271−280.
(17) Kansy, M.; Senner, F.; Gubernator, K. Physicochemical high throughput screening: parallel artificial membrane permeation assay in the description of passive absorption processes. *J. Med. Chem*. **1998**, *41*, 1007−1010.
(18) Wohnsland, F.; Faller, B. High-Throughput Permeability pH Profile and High-Throughput Alkane/Water log P with Artificial Membranes. *J. Med. Chem.* **2001**, *44*(6), 923−930.
(19) Nielsen, P. E.; Avdeef, A. PAMPA − a drug absorption in vitro model 8. Apparent filter porosity and the unstirred water layer. *Eur. J. Pharm. Sci*. **2004**, *22*(1), 33−41.
(20) Kubinyi, H. Lipophilicity and biological activity. *Arzneim.-Forschung./Drug Res*. **1979**, *29*, 1067−1080.
(21) Box, K.; Bevan, C.; Comer, J.; Hill, A.; Allen, R.; Reynolds, D. High-Throughput Measurement of pK_a Values in a Mixed-Buffer Linear pH Gradient System. *Anal. Chem.* **2003**, *75*(4), 883−892.
(22) Avdeef-A. *Absorption and Drug Development*: *Solubility, Permeability and Charge State*; John Wiley & Sons: New York, 2003; pp 59−66.
(23) *Sirius Technical Application Notes (STAN)*; Sirius Analytical Instruments Ltd.: Forest Row, RH18 5DW, U.K., 1996; volume 2, p 114.

JM049377W